30. Broecker, W. S. & Denton, G. *Geochim. cosmochim. Acta* **53,** 2465–2501 (1990).
31. Gordon, A. L. *J. geophys. Res.* **91,** 5037–5047 (1986).
32. Maier-Reimer, E. & Mikolajewicz, U. in *Oceanography* (eds Ayala-Castanares, A., Wooster, W. & Yanez-Arancibia, A.) 87–100 (UNAM, Mexico, 1989).
33. Cox, R. A., McCartney, M. J. & Culkin, F. *Deep-Sea Res.* **17,** 679–689 (1970).
34. Labeyrie, L. *et al. Quat. Sci. Rev.* (1992).
35. Broecker, W. S. *et al. Paleoceanography* **5,** 469–477 (1990).
36. Van Weering, T. C. E. & de Rijk, S. *Mar. Geol.* **101,** 49–69 (1992).

ACKNOWLEDGEMENTS. We thank E. Birchfield, E. Boyle, S. Calvert, J. Labrousse, H. Wang and R. Zahn for comments and suggestions, and J. Antignac, E. Kaltnecker, H. Leclaire, B. Le Coat and P. Maurice for help in the isotope and AMS analyses. This work is supported by the EEC, CEA, CNRS and INSU (PNEDC). T.C.E.v.W. was supported by NIOZ and SOZ.

Post-rifting stress relaxation at the divergent plate boundary in Northeast Iceland

G. R. Foulger*, C.-H. Jahn†, G. Seeber†, P. Einarsson‡, B. R. Julian§ & K. Heki*‖

* Department of Geological Sciences, University of Durham, Science Laboratories, South Road, Durham DH1 3LE, UK
† Institut für Erdmessung, Universität Hannover, D-3000 Hannover 1, Neinburger Strasse 5, Germany
‡ Science Institute, University of Iceland, Dunhaga 3, Reykjavik, Iceland
§ U.S. Geological Survey, 345 Middlefield Road, MS 977, Menlo Park, California 94025, USA

INTERACTION of the elastic lithosphere with the underlying anelastic asthenosphere causes strain to propagate along the Earth's surface in a diffusion-like manner following tectonism at plate boundaries. This process transfers stress between adjacent tectonic segments and influences the temporal tectonic pattern along a plate boundary. Observations of such strain transients have been rare, and have hitherto been confined to strike-slip and underthrusting plate boundaries[1]. Here we report the observation of a strain transient at the divergent (spreading) plate boundary in Iceland. A Global Positioning System survey undertaken a decade after an episode of dyke intrusion accompanying several metres of crustal spreading reveals a spatially varying strain field with the expected diffusion-pulse shape and an amplitude three times greater than the 5.7 cm that would be expected from the average spreading rate[2]. A simple one-dimensional model with a thin elastic layer overlying a viscous layer fits the data well and yields a stress diffusivity of $1.1 \pm 0.3\ m^2\ s^{-1}$. Combined with structural information from magnetotelluric measurements, this implies a viscosity of $0.3–2 \times 10^{19}$ Pa s—a value comparable to that derived for Iceland from post-glacial rebound[23], but low compared with estimates for mantle viscosity obtained elsewhere[3].

The Krafla volcanic system is one of five *en echelon* systems in the Northern Volcanic Zone of Iceland, the locus of the accretionary plate boundary there[4] (Fig. 1*a*). It comprises a 100-km-long fissure swarm containing the Krafla central volcano. The full spreading rate predicted by the NUVEL plate velocity model is 1.9 cm yr^{-1} (ref. 2).

A spreading episode commenced in the Krafla system in 1975 (refs 5–10). During the following decade a magma chamber beneath the volcano inflated, with occasional rapid deflations when magma flowed out of the chamber and was intruded along the fissure swarm, forming dykes. From 1975 to 1979, about 10 such deflations with dyke intrusion occurred. Terrestrial surveying work revealed that roughly a metre of local crustal widening accompanied each event. The total widening across the fissure swarm was ~2 m along 50 km of its length, and 6 m along another 30 km, giving an average expansion of 3.5 m (ref. 10). The average height of the dyke complex was estimated to be 2 km, assuming that its width was constant with depth[10]. The widening zone extended from Axafjordur in the north to Hverfjall in the south (Fig. 1*a*). Expansion in the centre of the fissure swarm was accompanied by contraction of the adjacent plates out to at least 50 km from the fissure swarm[11,12].

After 1980, most of the magma escaping during deflations flowed onto the surface as lava. Evidently the stress perpendicular to the plate boundary had increased so as to prevent further dyke intrusions. Post-intrusion earthquake focal mechanisms show the absence of a systematic extensional stress field, thereby supporting this conclusion[13,14].

Early geodetic studies indicate that little spreading occurred in the Krafla system during the 27-yr period 1938–65 (ref. 15). Historical records, however, describe eruptions and tectonism during the period 1724–29 that were similar to those of 1975–85. These observations suggest that crustal spreading is episodic in the Krafla system, with several metres of widening occurring during brief episodes of intense activity, separated by quiescent periods lasting hundreds of years.

A geodetic network of ~40 points encompassing Northeast Iceland was measured using the Global Positioning System

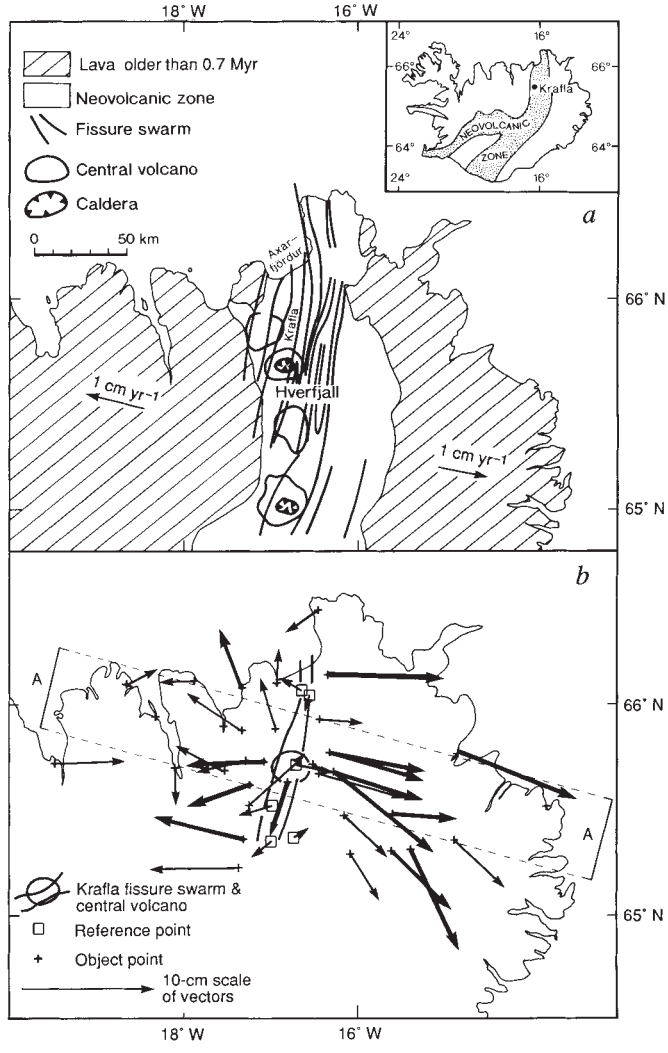

FIG. 1 *a*, Tectonic map of Northeast Iceland showing the five *en echelon* volcanic systems that comprise the accretionary plate boundary. *b*, Horizontal point displacements, 1987–90. The lengths of the vectors are proportional to the point displacements. Thick lines indicate vectors that are significant at greater than the 99% level (3σ). Zone A indicates the part of the network around the middle of the intruded dyke complex, and points within this zone are modelled in Fig. 2. Zone A extends from 26.5 km north of the point on Mount Krafla to 16.9 km south of it, parallel to the trend of the volcanic system.

‖ On leave from the Kashima Space Research Centre, Communications Research Laboratory, Japan.

(GPS) in 1987 and remeasured in 1990 (Fig. 1*b*). Points were concentrated within the Krafla volcanic system and were sparsely distributed for 130 km into the adjoining plates. In 1987 a six-satellite daily observation window 3 hr 20 min long was used, and most of the points were occupied two or three times. The data were processed at the University of Hannover with GEONAP (geodetic navstar positioning) software[16] and at the University of Durham with the Bernese version 3.2 GPS software[17]. The standard deviations of all the components are ~0.5–1.3 cm for the GEONAP results[15,18], and the integer values of all cycle slips and ambiguities could be calculated. The GEONAP and Bernese results agree to within 1 cm in the horizontal for more than 70% of the points. Broadcast ephemerides were used for both analyses, as the available precise orbits offered little improvement.

In 1990, a seven-satellite daily observation window of 4 hr 10 min was used[2]. Selective Availability (degradation of signal quality for military security) was on for most of the survey. The 1990 data are noisy because of ionospheric irregularities (scintillations) caused by the current sunspot maximum, but again, the integer values of cycle slips and ambiguities could be calculated using suitable linear combinations of the carrier-phase data. The 1990 GEONAP and Bernese solutions yielded standard deviations (1σ) of 1–3 cm for all components after network adjustment. The agreement between the GEONAP[19] and Bernese results is mostly within the 1σ error. We assumed a standard troposphere in all our analyses, an adequate model in the low-temperature environment of Iceland. Because of the great ionospheric turbulence, the 1990 results[18] are inferior to those from 1987.

The deformation results described here are based on the GEONAP results. The two coordinate sets with their complete variance-covariance matrices were subjected to deformation analysis using the PANDA[19] software. This corrected for systematic translations and rotations between epochs arising from unmodelled systematic errors using a set of reference points close to the rift axis that showed no significant scale deformation (Fig. 1*b*). The displacement field shows the relative motion of the other points (object points) with respect to the reference points. Significant movements occurred for 44% of the object points. The deformation field shows a large, systematic east–west expansion with a maximum amplitude of ~15 cm. This is clearest around the middle of the fissure swarm, where crustal widening was greatest during 1975–85 (zone A, Fig. 1*b*). Vertical movements were up to 10–15 cm, but no systematic deformation pattern such as occurs in the horizontal plane was observed.

The time-averaged spreading rate in Northeast Iceland, 1.9 cm yr^{-1} (ref. 2), cannot account for the deformation. Also, no significant tectonic activity occurred in our network between 1987 and 1990. We therefore attribute the 1987–1990 deformation to consequences of the 1975–85 spreading episode. We show below that the 1987–90 deformation agrees well with the field predicted for such an episode by the simple model of transient stress relaxation proposed originally by Elsasser[20] and Bott and Dean[21].

The Elsasser–Bott–Dean model consists of a thin elastic layer overlying a viscous layer (Fig. 2*a*). We will consider the deformation source as a long vertical dyke oriented in the y-direction, with x being the horizontal distance from the dyke and t being time. This problem is one-dimensional with the only non-zero component of horizontal displacement, $u(x, t)$, lying in the x-direction. If the traction exerted by the viscous layer on the base of the elastic layer is $-(\eta/b)\,\partial u/\partial t$, where η and b are the viscosity and thickness of the viscous layer, then u obeys the diffusion equation[20,21]

$$\frac{\partial u}{\partial t} = \kappa \frac{\partial^2 u}{\partial x^2} \tag{1}$$

with

$$\kappa = Mhb/\eta \tag{2}$$

where h is the thickness of the elastic layer and M is the elastic modulus relating horizontal stress and strain within it. For the plane-strain conditions assumed here (in the x–z plane), $M = 4\mu(\lambda+\mu)/(\lambda+2\mu)$, where λ and μ are the Lamé moduli. The elastic layer is initially at rest, and at time $t = 0$ a dyke of width $2U_0$ is intruded, so that the material immediately adjacent to the line $x = 0$ is suddenly displaced to the right or left by U_0. The appropriate solution to the diffusion equation (1) is[22]

$$u(x, t) = U_0 \operatorname{erfc} \frac{x}{2\sqrt{\kappa t}} \tag{3}$$

and the corresponding horizontal velocity is

$$\frac{\partial u}{\partial t} = \frac{U_0}{t\sqrt{\pi}} \frac{x}{2\sqrt{\kappa t}} e^{-x^2/4\kappa t} \tag{4}$$

We treat the observed 3-yr displacements as instantaneous velocity 11 years after the dyke intrusion episode, and estimate the half-width of the dyke, U_0, and the diffusivity, κ, by fitting the theoretical expression for the velocity, equation (4), to the observations.

Figure 2*b* illustrates the best-fit curve, in the least-squares sense, to the point displacements around the middle of the dyke

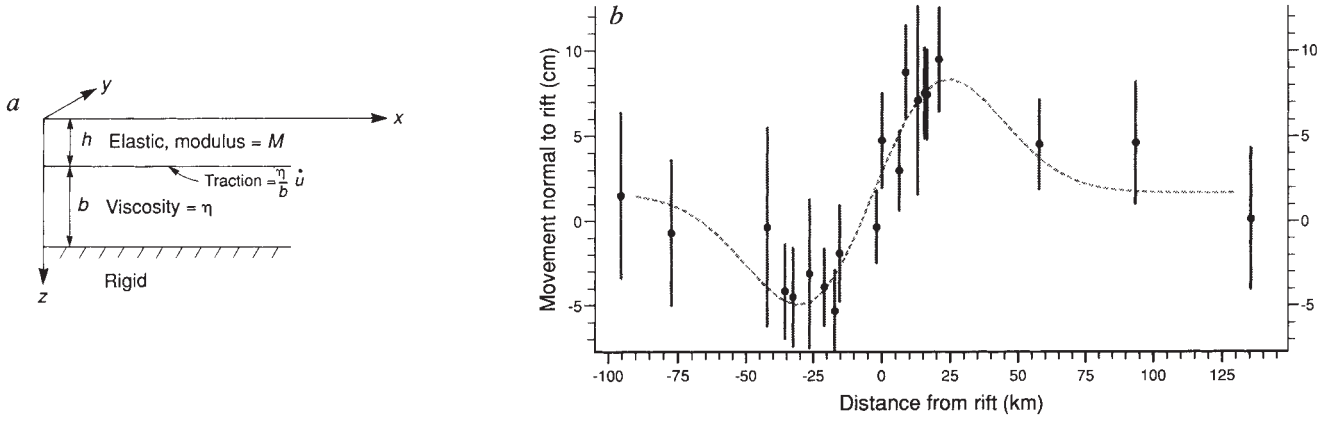

FIG. 2 *a*, Schematic diagram of the Elsasser–Bott–Dean model. *b*, Movements of points within zone A (Fig. 1*b*), perpendicular to the fissure swarm as a function of distance from it. The trend of the plate boundary is taken to be 015°. Vertical bars indicate 1σ error bars. The curve superimposed on the data points is the best-fit curve, in a least-squares sense, of the form predicted by the diffusion equation. It corresponds to a dyke half-width of 1.0 ± 0.1 m and a diffusivity of 1.1 ± 0.3 m^2 s^{-1}. This model has a normalized root-mean-square residual of 0.61 and a weighted root-mean-square residual of 1.68 cm.

complex, zone A (Fig. 1*b*). The position of the centre of the dyke is well known from previous geodetic measurements and was held to a fixed location within the fissure swarm. The analysis indicates a dyke half-width of 1.0 ± 0.1 m and a diffusivity of $1.1 \pm 0.3\ m^2\ s^{-1}$. This estimate of U_0 suggests a value of 2.0 m for the average width of the dyke complex, which is smaller than the 3.5 m obtained from geodetic measurements during the spreading episode, as expected if the dykes extend only part of the way through the elastic layer. The distance of the velocity maximum from the dyke, and therefore the value of the diffusivity obtained, $1.1\ m^2\ s^{-1}$, is fairly well constrained.

Equation (2) may be used to estimate the value of b, h or η, provided the two other parameters are assumed. Magnetotelluric work suggests that Northeast Iceland is underlain by a layer of partial melt 5–10 km thick, and it has been suggested that this layer decouples an overlying layer from material with a high viscosity below[10]. If we identify this partial melt layer with the viscous layer in our model, and take $h = 8$–30 km, $b = 5$–10 km, $\lambda = \mu = 0.28 \times 10^{11}$ Pa for basalt and $\kappa = 1.1\ m^2\ s^{-1}$, we calculate $\eta = 0.3$–2×10^{19} Pa s. This may be compared with values of 10^{19} Pa s obtained for the viscosity in a half-space model of Icelandic post-glacial rebound[23].

The rebound estimate of viscosity is not significantly different from ours. Our estimate of diffusivity, however, is incompatible with a thick layer having a viscosity as low as we have calculated. These two apparently incompatible results can be reconciled by a model that involves a thin, shallow layer of relatively low viscosity ($\ll 10^{19}$) underlain by a thicker layer of higher viscosity ($\sim 10^{19}$). The thin, shallow layer may lubricate horizontal motions in the manner suggested by Bjornsson[10] and at the same time transmit stress from the large-scale glacial relief to deeper regions.

Our model is a simplification, and although the data have the essential shape predicted by diffusion theory, our quantitative interpretation should be viewed as tentative. Our assumption of one-dimensionality overestimates the motion at distant points, although this effect is small for points close to the dyke, which dominate our values of U_0 and κ. Ignoring the effect of older transients underestimates the motion at distant points. The radial component of the deformation field apparent in Fig. 1*b* results from the real two-dimensionality of the dyke. We assume thinness and perfect elasticity for the upper layer, newtonian behaviour for the lower layer and lateral homogeneity. These approximations probably have a significant effect on the value that we calculate for the diffusivity, κ, and thus viscosity, η. A model incorporating viscoelasticity and finite layer thicknesses would result in modified values.

Of the three stages of the 'seismic cycle' (strain accumulation between events, co-seismic elastic step and post-seismic transient), the strain transient is the least well observed. But transient behaviour contains unique information about the structure and rheology of the Earth and its response to stress changes. In addition, it influences the temporal interactions of earthquakes. Transient stress diffusion is a physical mechanism by which the stress changes accompanying an earthquake or rifting episode are redistributed to adjacent regions and contribute eventually to triggering other earthquakes. Statistical analyses of the spatial and temporal correlations between earthquakes have had little success in predicting their behaviour. A physical model that incorporates both co-seismic elastic and delayed transient stress redistribution may be a better prediction tool.

Observations of transients from spreading plate boundaries are particularly difficult to acquire because most of the world's rift system is on the ocean floor. A similar but smaller dyke intrusion event in 1978 in the rift system of Afar, East Africa, was studied geodetically[24–26]. The deformation following the intrusion is compatible with that from Northeast Iceland. The network in Afar, extending to 37 km from the rift, was however too narrow to detect any but the quasi-linear central part of the stress diffusion curve, and the observations were interpreted as a steady state process controlled by the plate motion. Reinterpretation of the Afar observations in terms of transient stress diffusion would be expected to yield insights into the structure and rheology of this area. □

Received 24 February; accepted 16 June 1992.

1. Thatcher, W. *J. geophys. Res.* **88,** 5893–5902 (1983).
2. DeMets, C., Gordon, R. G., Argus, D. F. & Stein S. *Geophys. J. int.* **101,** 425–478 (1990).
3. Cathles, L. M. III *The Viscosity of the Earth's Mantle* (Princeton Univ. Press, 1975).
4. Saemundsson, K. *Geol. Soc. Am. Bull.* **85,** 495–504 (1974).
5. Bjornsson, A., Saemundsson, K., Einarsson, P., Tryggvason, E. & Gronvold, K. *Nature* **266,** 318–323 (1977).
6. Bjornsson, A., Johnsen, G., Sigurdsson, S. & Thorbergsson, G. *J. geophys. Res.* **84,** 3029–3038 (1979).
7. Brandsdottir, B. & Einarsson, P. *J. Volcanol. geotherm. Res.* **6,** 197–212 (1979).
8. Einarsson, P. & Brandsdottir, B. *J. Geophys.* **47,** 160–165 (1980).
9. Johnsen, G. V., Bjornsson, A. & Sigurdsson, S. *J. Geophys.* **47,** 132–140 (1980).
10. Bjornsson, A. *J. geophys. Res.* **90,** 10151–10162 (1985).
11. Moller, D. & Ritter, B. *J. Geophys.* **47,** 110–119 (1980).
12. Moller, D., Ritter, B. & Wendt, K. *Earth Evol. Sci.* **2,** 149–154 (1982).
13. Foulger, G. R., Long, R. E., Einarsson, P. & Bjornsson, A. *Nature* **337,** 640–642 (1989).
14. Arnott, S. A. thesis, Univ. Durham (1990).
15. Jahn, C.-H., Seeber, G., Foulger, G. R. & Bjornsson, A. *Proc. int. Assoc. Geodesy Symp. 101 Edinburgh, 1989* (eds Vyskocil, P., Reigber, C. & Cross, P. A. (Springer, New York, 1989).
16. Wuebbena, G. in *Proc. 5th int. Geodetic Symp. Satellite Positioning* Las Cruces, New Mexico (1989).
17. Rothacher, M., Beutler, G., Gurtner, W., Schildknecht, T. & Wild, U. *Bernese GPS Software Version 3.2* (Univ. Bern, 1990).
18. Jahn, C.-H., Seeber, G., Foulger, G. R. & Einarsson, P. *IUGG Symp. U5, AGU Monogr. Series 1992* (in the press).
19. Wanninger, L. & Jahn, C.-H. in *Proc. IAG Symp. G-2* (ed. Mader, G. L.) (Springer, Heidelberg, 1992).
20. Elsasser, W. M. in *The Application of Modern Physics to the Earth and Planetary Interiors* (ed. Runcorn, S. K.) 223–245 (Wiley, London, 1969).
21. Bott, M. H. P. & Dean, D. S. *Nature* **243,** 339–341 (1973).
22. Carslaw, H. S. & Jaeger, J. C. *Conduction of Heat in Solids* (Oxford Univ. Press, 1959).
23. Sigmundsson, F. *Geophys. Res. Lett.* **18,** 1131–1134 (1991).
24. Abdallah, A. *et al. Nature* **282,** 17–23 (1979).
25. Ruegg, J. C., Kasser, M. & Lepine, J. C. *J. geophys. Res.* **89,** 6237–6246 (1984).
26. Ruegg, J. C. & Kasser, M. *Geophys. Res. Lett.* **14,** 745–748 (1987).

ACKNOWLEDGEMENTS. In addition to those who contributed to collecting and processing the GPS data, we thank F. Holliday, M. H. P. Bott, J. Savage, W. Thatcher, P. Seagall, W. Prescott, J. Morgan and P. England for their advice and help. The contribution of the University of Hannover was financed by DFG. The contribution of the University of Durham was financed by NERC and the Wolfson Foundation. This research was helped by the University of Durham Computer Service, and by their experimental Internet connection.

Ridge segmentation, faulting and crustal thickness in the Atlantic Ocean

Peter R. Shaw

Woods Hole Oceanographic Institution, Woods Hole, Massachusetts 02543, USA

THE Mid-Atlantic Ridge (MAR) between the Kane and Atlantis fracture zones consists of segments 20–85 km in length[1]; bull's-eye patterns in the mantle Bouguer gravity anomaly field[2] centred on several segments associated with narrow rift valleys[3] have been interpreted as centres of strong mantle upwelling and thick crust. Here I present a map of normal faults inferred from $\sim 5 \times 10^4$ km^2 of Sea Beam bathymetry[4] along the MAR between 28° N and the Atlantis fracture zone. Faults are mapped both on- and off-ridge using a criterion that distinguishes them from volcanic topography. Abyssal hill lineations seem to form at the rift valley walls through the growth of the normal faults; towards ridge segment ends these faults are more widely spaced, with larger throws than those at segment centres, and often define the boundaries of the gravity bull's-eyes. These two different faulting styles, which probably reflect changes in lithospheric strength, are preserved into the rift mountains. Large-throw faults are highly correlated with the mantle Bouguer highs, suggesting that amagmatic extension on the large faults contributes to the crustal thinning inferred towards the segment ends.

To distinguish faults from constructional volcanism, both of which can create steep slopes, I measure topographic curvature